



Salem, A. M., Zaini, I. N., Paul, M. C. and Yang, W. (2019) The evolution and formation of tar species in a downdraft gasifier: numerical modelling and experimental validation. *Biomass and Bioenergy*, 130, 105377. (doi:[10.1016/j.biombioe.2019.105377](https://doi.org/10.1016/j.biombioe.2019.105377))

There may be differences between this version and the published version. You are advised to consult the publisher's version if you wish to cite from it.

<http://eprints.gla.ac.uk/197025/>

Deposited on: 19 September 2019

Enlighten – Research publications by members of the University of Glasgow
<http://eprints.gla.ac.uk>

The Evolution and Formation of Tar Species in a Downdraft Gasifier: Numerical Modelling and Experimental Validation

Ahmed M. Salem^{a,b}, Ilman Nuran Zaini^c, Manosh C. Paul^{a,*}, Weihong Yang^c

^aSystems, Power and Energy Research Division, James Watt School of Engineering,
University of Glasgow, Glasgow, G12 8QQ, UK

^bMechanical Power Department, Faculty of Engineering, Tanta University, Egypt

^cKTH Royal Institute of Technology, Stockholm 100 44, Sweden

*Corresponding author: Manosh.Paul@glasgow.ac.uk; +44(0)141 330 8466

ABSTRACT

Gasification is one of the most important methods for converting biomass to syngas currently used in energy production. However, tar content in syngas limits its direct use and requires additional removal techniques. The modelling of tar formation, conversion and destruction along a gasifier could give a wider understanding of the process and help in tar elimination and reduction. However, tar complexity, which contains hundreds of species, makes the modelling process hard and computationally intensive, because the chemistry of the formation and the combustion of many species have not yet been fully studied. In this work, a detailed kinetic model for the evolution and formation of tar from downdraft gasifiers, for the first-time, was built. The model incorporates four main tar species (benzene, naphthalene, toluene, and phenol) with a total of eighteen different kinetic reactions implemented in the code for every zone. Experimental work was carried out to initially validate the results of the kinetic code and found a good agreement. Further experiments were conducted at three different equivalence ratios (ER) and at three different temperatures (800, 900, and 1100 °C). Sensitivity analysis was then carried out by the kinetic code to optimise the working parameters of a downdraft gasifier that led to a higher calorific value of syngas. The results reveal that a tar evolution model is more accurate for wood biomass materials and that using ER around 0.3, and moisture content levels lower than 10% lead to the production of higher value syngas with lower tar amounts.

Keywords: Biomass gasification; Downdraft gasifiers; Tar species; Numerical modelling; Thermochemical kinetics; Gasification experiment

1. Introduction

Biomass, as an energy source, is a promising alternative to fossil fuels. In addition, it is a clean and renewable source of energy and is environmentally friendly. Energy production from biomass can be done through combustion, gasification, pyrolysis and torrefaction. Gasification of biomass yields three main products: gases, solids, and condensable tars [1]. Useful gases produced from gasification are mainly CO, H₂, and CH₄, with undesired gases such as N₂, and CO₂ plus considerable amounts of tar compounds [2], [3], and [4]. Tar particularly causes serious problems in any direct downstream application of producer gases from gasification. For example, it can cause blockage of gas downstream, fouling and erosion for equipment. In addition, tar formation wastes some of the effective energy from biomass gasification [5].

An effective way to use syngas directly as a fuel is to limit the formation of tar or reduce it to a specific level. Therefore, studies have been particularly focused on investigating the nature of the formation and destruction of tar compounds. However, experimental studies regarding tar formation and destruction are a cost and time consuming process. On the other hand, tar involves complex compounds as it could form in hundreds of different chemical compounds [1], and because of this, many researchers only considered it as a single compound ($C_6 H_{6.62} O_{0.2}$) [6], while others mainly took into account the formation of Poly-Aromatic Hydrocarbons (PAH) [7]. Another effective technique to study the tar compounds' formation in gasification processes is modelling either by thermochemical kinetics (e.g. see [7] and [8]) or by computational fluid dynamics (CFD) modelling (e.g. see [9], and [10]). This work extends the downdraft gasification modelling [6] by including a set of new kinetic mechanisms for specific tar compounds.

Previously, researchers ([11], [12], and [13]) used equilibrium models based on one global reaction mechanism and succeeded in predicting the product gas composition and gasification temperature to some extent. While other researchers used multi-step equilibrium models [14] in order to improve the accuracy of the prediction, the equilibrium models are less effective and give an over prediction for the gas production and tar content [15]. Thermodynamic equilibrium models also fail to take into account the physical and multi-step chemical phenomena inside a gasifier, thus originating errors in some species estimation [16].

On the other hand, kinetic models are used to simulate gasifiers more accurately with a wide range of controlled parameters and outcomes (e.g. producer gas composition, temperature profile, heating value and gasifier dimensions) [6], and [17]. Computational fluid

dynamics (CFD) models has no contribution in tar formation during downdraft biomass gasification, ([9] , and [18]) .Some kinetic models have also been used to predict the tar formation during biomass gasification (e.g. see [1] , [19], and [20]), where tar was simply defined as a hydrocarbon that has a molecular weight greater than benzene (C_6H_6) [19]. However, tars could form in hundreds of different chemical compounds, but in most cases, approximately twenty species are considered to have significant amounts [1].

Further, simple models built for the tar modelling using one single-compound representing all the tar species are assumed to give the tar amount as a percentage of the total gas production [6], where $C_6H_{6.62}O_{0.2}$ was used as a tar representative compound, whereas Liu et al. [21] used steam reforming of toluene as a biomass tar model compound to study the tar destruction process using a gliding arc technology. Zhao et al. [22] also used toluene in the tar steam reforming modelling during the pyrolysis of biomass. Toluene was chosen particularly for its stability and because it gave a good representation of tar produced during pyrolysis. Other compounds such as phenol were used in the modelling of air-blown gasifiers [23], considering the formation of phenol as a primary tar.

A detailed kinetic model was presented by Dufour et al. [16] for the tar formation in dual fluidized bed gasifiers (DFB). They used four main lumped compounds representing ten tar species in their modelling based on the correlations and kinetic reactions inside the gasifier. Aspen plus modelling code was used, and the model was used to optimise the DFB gasifier's working condition. Palma [7] also developed a kinetic model for tar evolution also in fluidized bed gasifiers. The results were compared with the experimental data and found good agreement for some species; however it overestimated tars of Class 2 and total tar concentration. Corella et al. [24] built a lumped model with six tar groups. The groups were benzene, one-ring compounds, naphthalene, two-ring compounds, three to four-ring compounds and phenolic compounds. They used a set of six different kinetic equations with eleven kinetic constants to model tar formation and cracking in fluidized bed biomass gasifiers. They found that Phenolics are most likely to be formed while naphthalene was hard to crack.

Other models were used to predict the tar formation during biomass gasification (e.g. [25]-[26]). It appeared that few studies about the detailed tar modelling in downdraft gasifiers have been done recently and most studies mainly focused on the syngas production, because tars are difficult to analyse and sample compared to the other gases. As a result, a novel aspect of this work is that it shows a detailed kinetic code for the modelling of tar and gas species formation along the downdraft gasifiers in one code.

The current work is a combination of modelling and experimental validation for the tar species evolution in air-blown downdraft gasifiers. A tar evolution model is built and combined with an existing model developed recently by the authors [6] – a four-zone integrated kinetic model allowing prediction of the optimum working parameters of a downdraft gasifier. The model was tested and verified over a wide range of biomass materials. The model has been used currently to optimise gasification and pyrolysis of biomass [27]. This paper presents an extension of the model through the implementation of four main tar species instead of one general compound. Tar species evolution will be tracked along the gasifier height from pyrolysis to oxidation and reduction zones. A good understanding of the evolution of different gas species and tar, and their relationship to temperature at each zone and other working parameters, will be of great importance when designing a gasifier and also in reducing tar content in producer gas. The results can be used to optimise the work of downdraft gasifiers that lead to the production of higher value syngas. There seems to be no other kinetic model that includes tar formation tracked from each zone, and their influence on the production of different gas species along a downdraft gasifier height at different zones.

2. Based on the review made, the novelty in the current research work is addressed through building up a kinetic code for simulating downdraft air-blown gasifiers. The code is totally built by authors using Matlab coding and does not depend on any external modeling codes (e.g. Aspen, or ANSYS). Additionally, Most of earlier published works only takes into account tar formation as a total amount or selected species [28], but the current model predicts the formation of detailed tar species based on kinetic rate reactions along gasifier height and at the exit with producer gas which has never been mentioned earlier. Experimental Setup

2.1. Gasification unit

A pilot-scale gasification unit designed for gasification, combustion and pyrolysis of different feedstocks using air and/or steam mixtures was used. A schematic view of the test rig is shown in Figure 1. The combustor is an axial cylinder surrounded by a heater connected to a control panel which can heat up to 1423 K. The system is connected to a water/isopropanol path to collect tar generated (Figure 2a) followed by a filter for tar and particulates removal, then gas flows to a micro GC system to analyse the syngas. The sample boat/holder is 10 cm length, while the internal combustor diameter is 24 cm, surrounded by a heater of 1.5 mm thickness. The axial combustor length is 50 cm, while the total length of the test rig is 100cm.

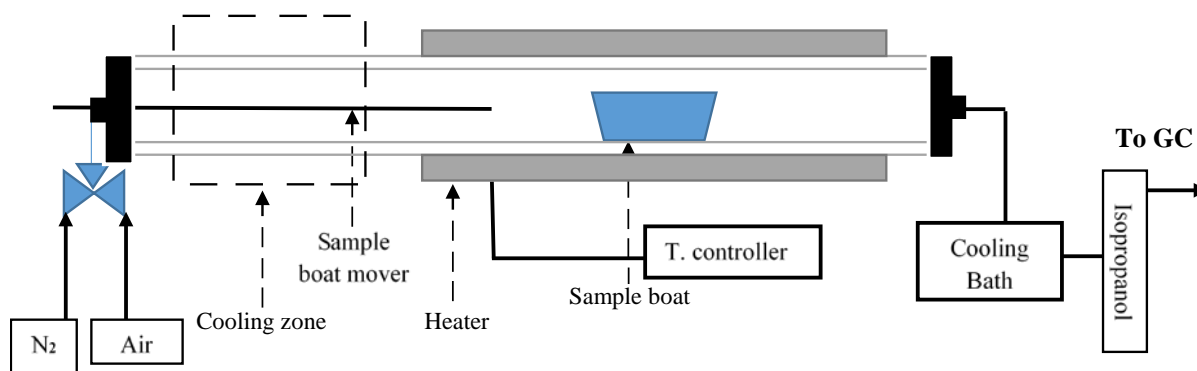


Figure 1. Schematic diagram of gasification test rig used in experiments.

Two thermocouples were connected to the system. The first was connected to the heater that was controlled by the control panel, while the second thermocouple was connected to the sample holder to measure the temperature of gasification during the experiment.

2.2. Materials and feedstocks' preparation

Wood was used as a feedstock with the ultimate analysis shown in Table 1. Lignocellulose biomass from beech wood was used as a feedstock with the ultimate analysis shown in Table 1. The wood sample was purchased from J. Rettenmaier & Söhne GmbH, Rosenberg, Germany. It was received in the form of fine particles (particle size ranged between 150 – 500 μm), and used directly in experiments after drying. The analysis was carried out by BELAB AB, Sweden [29]. Samples were first dried in an oven for twenty-four hours at 373 K to reduce the amount of water content, since dry samples have the advantage of easier tar sampling and analysis. Three different equivalence ratios (ER) were used (0.25, 0.3, and 0.35) at three different temperatures (1073, 1173, and 1273 K).

Table 1: Biomass analysis of feedstocks used [29].

Ultimate Analysis, db	
C	49.1
H	6.1
O	43.8
N	0.12
S	0.026
Ash	0.8
Moisture% wt	14.1
Vol. %, db	84.2
Gross CV, MJ/kg	16.884

2.3. Experimental procedure

After drying samples in the oven, a sample holder was filled with a sufficient amount of wood (4.7g). The sample holder was weighed before and after the sampling to measure the accurate amount of sample. A specific scale was used for weighing the samples and bottles with an accuracy of 0.001 g. Glass bottles for tar collection were washed and dried and their weight was measured individually. The inner tube of the reactor was cleaned by methanol to ensure that there was no tar or ash inside. The temperature of the experiment was then set by the control panel which heats up the system at a rate of 35 degrees/min. Nitrogen was also used for a leakage test to ensure there was no gas leakage from the system. The sample was then placed at the start of the reactor tube (at around 423 K). The amount of air based on the required ER was calculated and nitrogen was fed first to ensure that no air remained in the reactor. Air amount for every run was calculated based on the ER wanted, and for 40 min experiment time it was supplied through three way valve and been adjusted using air flow meter.

The tar collection bottles were immersed inside the bath of the cooler at a temperature of 253 K. This temperature is below the condensation temperature of all the well-known tar species. The air flowrate was adjusted by a flowmeter based on a specific residence time of the experiment to ensure a sufficient amount of gasification medium based on the calculations of ER. When the temperature inside the tube reached the required experiment temperature, the sample holder was pushed to the middle of the reaction tube and air replaced nitrogen. The temperature and time were recorded for every run.

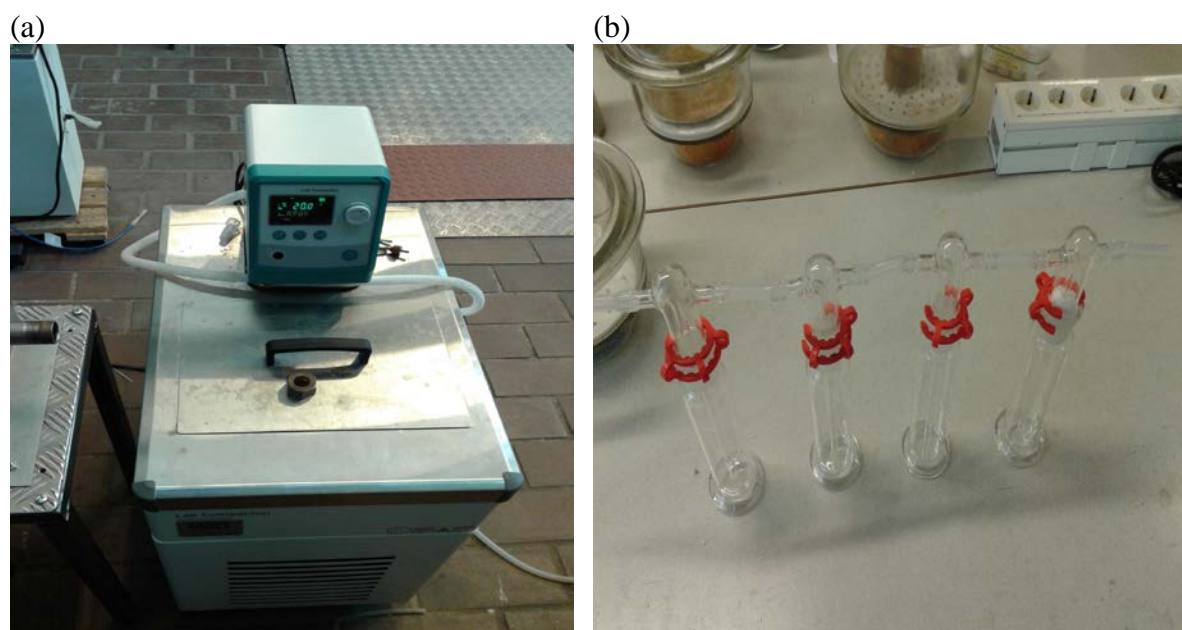


Figure 2. (a) Cooler bath used to condense tar, and (b) glass bottles used to collect tar samples

Once the sample was placed in the middle of the reactor and air flows, tar started to form and was collected in the bottles and syngas continued to flow to be analysed in the micro-GC system. Heavier tar molecules were collected in the first bottle followed by lighter molecules in the following bottles. The last bottle had a specific filter followed by a bottle filled with isopropanol followed by a filter to remove all particulates and tars before being analysed in the gas chromatograph.

2.4. Tar sampling and Solid Phase Adsorption (SPA) method for tar analysis

In Figure 3(a), condensed tar species in the bottles is shown for wood fibre gasification at 1173 K, for an ER of 0.3. After collecting tar, it is further diluted using Dichloromethane (DCM) in order to be analysed and to give a tar species concentration. Figure 3(a) shows heavier tar compounds (darker colours) collected in the first bottle, followed by lighter compounds in the following bottles. Condensation takes place as a result of lower bath temperature (253 K). Bottles are then weighed after each run to measure the total amount of tar produced.

Tar collection as shown in Figure 3(b) in order to identify detailed tar species in the tar produced from the gasification of biomass. The tar collected in 100 ml of syngas was sent to be further analysed using the SPA method. A specific syringe with 100 ml internal volume is used for collecting tar inside this volume where the gas coming out of the system is subjected to the syringe until it is totally filled.

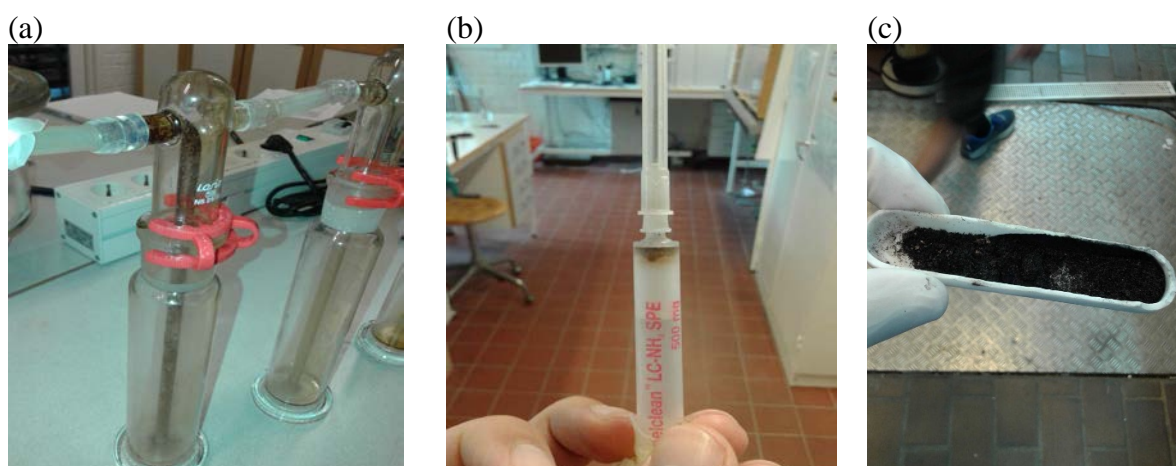


Figure 3. (a) Tar collected in bottles, (b) tar collection by SPA method syringe, (c) ash collected after the experiment.

The detailed SPA (Solid Phase Adsorption) method is an offline collection method used to analyse tar compounds. It is used to detect and analyse tar compounds that have a boiling point up to 673 K which is sufficient for most gasification applications as the gasifier temperature is obviously higher than that [30]. With a rapid sampling time (around 1 minute), a wide range of aromatic and phenolic compounds can be detected in μg for every 100 ml of gas.

Tar is collected in the gas phase (523-573 K) by being trapped in a small disposable polypropylene column in a small syringe with the help of a 100 ml syringe (Figure 3(b)) Tar is later analysed by a gas chromatograph (Varian CP-3800) with a flame ionization detector (FID). The main compounds detected by this method are shown in Table 2.

Table 2: Detectable compounds of SPA tar collection method

Aromatics	Phenolics
Benzene	Phenol
Toluene	o-Cresol
m/p-Xylene	m-Cresol
o-Xylene	p-Cresol
Indan	2,4-Xylenol
Indene	2,5/3,5-Xylenol
Naphthalene	2,6-Xylenol
2-Methylnaphthalene	2,3-Xylenol
1-Methylnaphthalene	3,4-Xylenol
Biphenyl	
Acenaphthylene	
Acenaphthene	
Fluorene	
Phenanthrene	
Anthracene	
Fluorantene	
Pyrene	

Ash content after the experiment is shown in Figure 3(c) which ensures that the sample amount is gasified.

3. Numerical Model

A detailed kinetic code for the tar evolution and destruction is built and combined with the kinetic code previously developed by the authors [6]. The model uses a set of kinetic rate reactions and balance equations for the different zones of a downdraft gasifier. The kinetic code is able to predict the downdraft gasifier performance through a wide range of output variables and control parameters. The model is also able to predict the producer gas

composition, temperature variations along the gasifier height, velocity and pressure variations, gasifier design and tar formation as a one general compound. The model was tested and verified over a wide range of materials and working parameters against well-known experimental data and further used to optimise the downdraft gasifier work based on a sensitivity analysis [6]. Further details on the methodology related to the development and verification of the kinetic model are available in the earlier published work of the authors, see [6].

In this work, four main tar species were added to the model to represent tar formation using detailed kinetic reactions. The yield of tar species at different zones of a gasifier is discussed based on the temperature of each zone. Mass and energy balances are calculated. Eighteen different kinetic reactions are implemented in the kinetic code to predict the optimum working conditions that lead to the production of a higher value producer gas. More details of the model are presented in [31].

Tar species evolution will be tracked from the pyrolysis to oxidation and reduction zones. A good understanding of the evolution of different gas species and tar, and their relationship to the temperature at each zone and other working parameters, will help to reduce the tar content in producer gas and also be of great importance when designing a gasifier. The results will also discuss the optimum working parameters that lead to the production of higher value syngas.

3.1 Pyrolysis sub-model

Tar decomposition based on the pyrolysis temperature is addressed and discussed in the present work. Ref. [8] reported parameters for the empirical correlations of pyrolysis products, as shown in Table 3, based on the experimental data taken from [32] which gives the mass yield of tar evolution during the pyrolysis process in g tar/ kg biomass.

Table 3: Correlations for pyrolysis products [8]

	<i>a</i>	<i>b</i>	<i>c</i>
C₇H₈	-6E-5	0.10701	-48
C₁₀H₈	-0.0001	0.218	-115.32
C₆H₆	-0.0003	0.7017	-387.6
C₆H₆O	2E-5	-0.068	46.42

The mass yield of different tar species *Y*, in g/kg biomass, can be derived by using the following equation:

$$Y = aT^2 + bT + c \quad (1)$$

After calculating the mass yield of the four main tar species at the pyrolysis zone, they are added to the pyrolysis products and an energy balance is carried out in order to calculate the pyrolysis temperature through equation (2).

$$\sum X_i \cdot (h_f + C_p \cdot \Delta T)_{pyrolysis\ products} = \sum X_i \cdot (h_f + C_p \cdot \Delta T)_{combustion\ products} + Q_{loss} \quad (2)$$

The heat loss is mentioned in the oxidation zone only because it is at a higher temperature than in the other zones and the overall heat loss is 10% of the product of the equivalence ratio and HHV [20]. The same energy balance principle is made for every zone in order to get the corresponding temperature.

After calculating the temperature, a backward calculation is made to give the exact gas composition for the pyrolysis products including the tar species.

3.2 Tar species in combustion and reduction zones

The products of pyrolysis are used as a feed to the oxidation zone. The reactions stated in Table 4 are implemented in the kinetic model for both the combustion and reduction zones. These reactions are taken from the references mentioned in the Table. Other reactions for the gasification and combustion were already discussed in [6] and will not be repeated here.

Table 4: Reactions of tar species implemented in the model.

	Reactions and rate expression	$A \text{ (s}^{-1}\text{)}$	$E \text{ (kJ/mol)}$	Ref
1	$C_7H_8 \rightarrow 0.17C_{10}H_8 + 0.89C_6H_6 + 0.67H_2$ $r_1 = k_1 [C_7H_8]$	2.23E13	315	[33]
2	$C_{10}H_8 \rightarrow 10C + 4H_2$ $r_2 = k_2 [C_{10}H_8]^2 [H_2]^{-0.7}$	5.56E15	360	[34]
3	$C_{10}H_8 + 4H_2O \rightarrow C_6H_6 + 4CO + 5H_2$ $r_3 = k_3 [C_{10}H_8] [H_2]^{0.4}$	1.58E12	324	[34]
4	$C_7H_8 + H_2 \rightarrow C_6H_6 + CH_4$ $r_4 = k_4 [C_7H_8] [H_2]^{0.5}$	1.04E12	247	[34]
5	$C_6H_6 + 5H_2O \rightarrow 5CO + CH_4 + 6H_2$ $r_5 = k_5 [C_6H_6]$	4.4E8	220	[34]
6	$C_6H_6 + 7.5O_2 \rightarrow 6CO_2 + 4H_2O$ $r_6 = k_6 [C_6H_6]^{-0.1} [O_2]^{1.25}$	17.83	125.5	[34]
7	$C_6H_6 + 3O_2 \rightarrow 6CO + 3H_2$ $r_7 = k_7 [C_6H_6] [O_2]$	1.58E15	202.6	[34]
8	$C_7H_8 + 9O_2 \rightarrow 7CO_2 + 4H_2O$ $r_8 = k_8 [C_7H_8]^{-0.1} [O_2]^{1.25}$	14.26	125.5	[34]
9	$C_6H_6O \rightarrow CO + 0.4C_{10}H_8 + 0.15C_6H_6 + 0.1CH_4$ $\quad \quad \quad + 0.75H_2$ $r_9 = k_9 [C_6H_6O]$	1.0E7	100	[8], [35]

4. Results and Discussion

4.1 SPA tar results

Tar samples are collected and further analysed in order to obtain detailed tar species as presented in Figure 4.

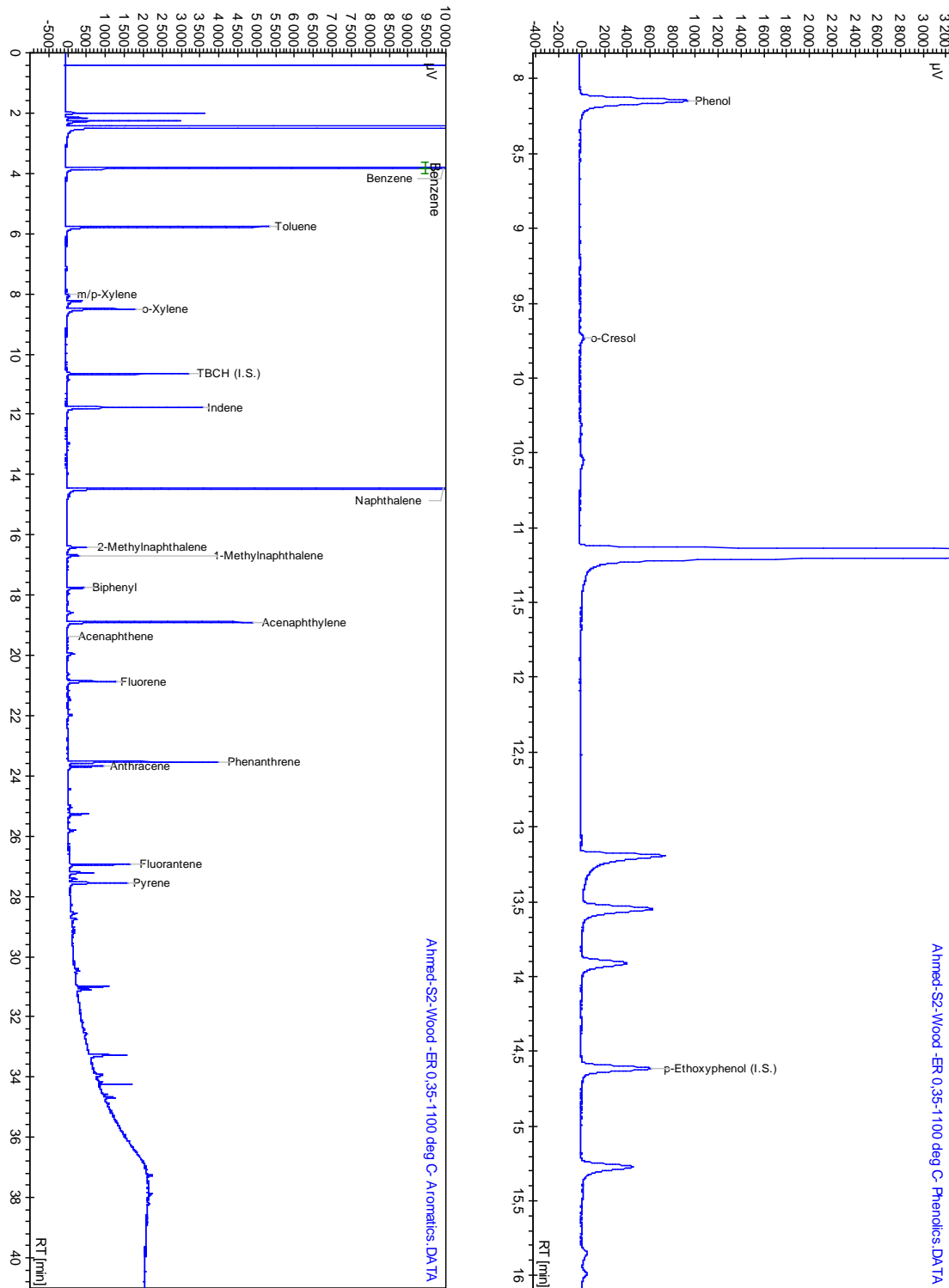


Figure 4. Tar species released during GC analysis of tar from wood sample obtained

through the SPA sampling method.

The results in Figure 4 illustrate the area covered by the different aromatic and phenolic species for wood sample gasification. The experiment was carried out at an ER of 0.35 and temperature of 1273 K and the results are further converted to amount (μg) per 100 ml of syngas. Further, GC analysis was performed to confirm the retention time for tar species. Based on the literature [1], hundreds of tar species can be detected. However, in the present work, only twenty-six species were found in significant amounts, varying between aromatics (such as benzene, naphthalene and xylene) and phenolics (such as phenol and cresol). Under all the working conditions and changing parameters (MC, ER), it was seen that the tar species selected are always in large amounts of approximately 70-95%. The concentration of remaining tar species (such as xylene, indene, pyrene, cresol and xylenol) can be ignored as a result of having a very small amount or a lack of chemical data and kinetic rate reactions that can help in building a stable kinetic code.

4.2 Model validation

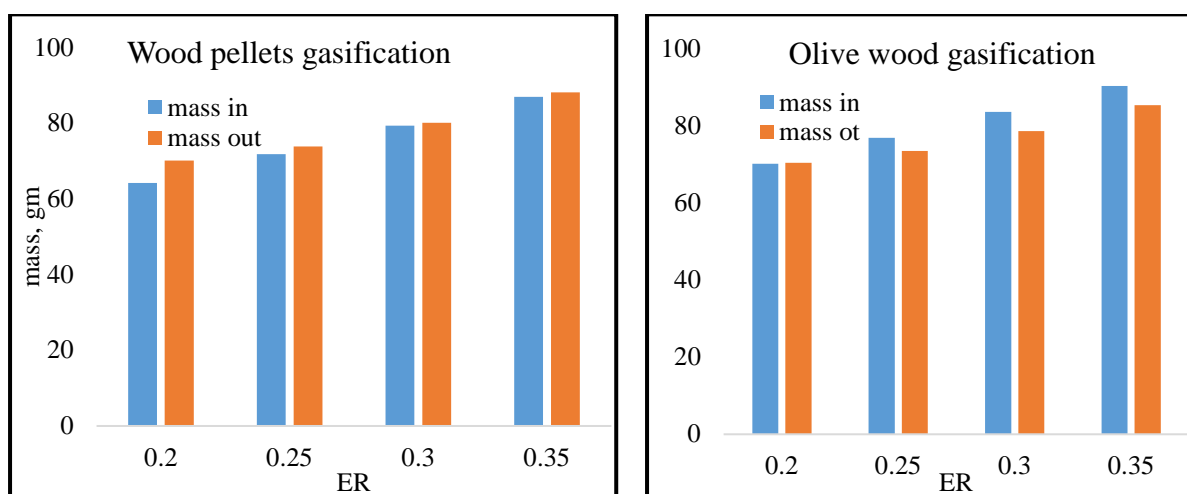


Figure 5. Mass balance calculations for different feedstocks.

Figure 5 shows the mass balance calculations for wood pellets and olive wood at different equivalence ratios with a constant moisture content of 10% for the results derived from the kinetic code. These calculations are based on the numeric results driven from the kinetic code. Total mass input, including biomass and air, is calculated and the mass output includes the producer gas and tar species. Unlike an equilibrium model that should give the exact results for the mass balance, the kinetic code which depends on many variables (e.g. the zones temperature, gas species concentration and gas velocity) are expected to have slight

variations between the mass input and output. However, this discrepancy has to be within a specific and acceptable limit. The results presented tend to be fair although a slight variation is found at a lower equivalence ratio for wood pellets which might be because of the lower air content that leads to a mass decrease compared to that of the higher ERs. However, the results look stable (1-8 % variations), and show the model's stability at different working conditions such as the equivalence ratio.

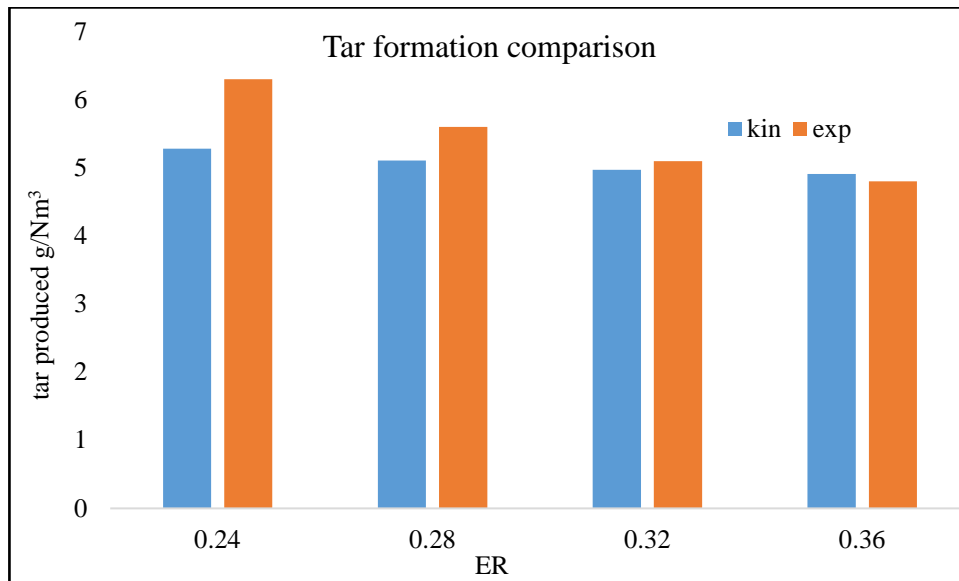


Figure 6. Total tar formation comparison between the present model and experimental results [36].

The comparison shown in Figure 6 between the results obtained by the present model and the other experimental data [36], demonstrates a good agreement for the total tar amount. The model is following the same boundary conditions used in experiments for correct validation, where MC is fixed 6.17% and ER is varied from 0.24-0.36. Maximum tar produced by the model shows values approximately 5 g/Nm³ and it is also in agreement with [37], where they stated that tar produced in downdraft gasifiers is in the range of 0.01-6 g/Nm³. In the experimental work of [36], they used corn stalks with a moisture content level of 6.17%, and the comparison is made for the different values of the air equivalence ratio to measure stability of current model for a normal range of working conditions.

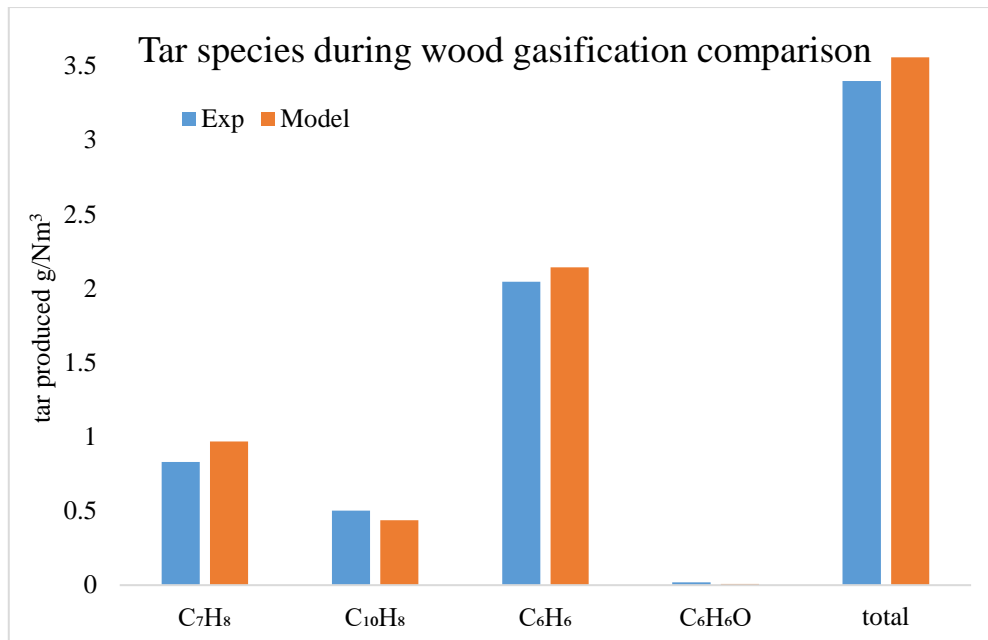


Figure 7. Tar species validation for wood gasification ER 0.35.

The set of results presented in Figure 7 show the tar species produced during the gasification of wood at an ER of 0.35. Comparisons are made between the results from the numerical model and the corresponding tar collected by the SPA method. Tar amounts are shown in $\mu\text{g}/100\text{ml}$ of syngas produced as given in the experimental results and comparison is made at the same gasification temperature of model and experiments (1173 K). Experiments were carried out at different gasification temperatures, while model results showed that wood gasification temperature at ER of 0.35 will be around 1158K which can be assumed to be very close to the experimental temperature used. The results show reasonably good agreement for all the major tar species produced and also for the total tar amount. Phenol concentrations are too small and can be considered as negligible compared to other species because, it is a primary tar compound that tends to be fully cracked and converted to other species at higher temperatures. The experiment is carried out at axial combustor and the modeling considering downdraft gasifiers. However, the model is relying on the detailed kinetic rate reactions that do not depend on the gasifier geometry, and hence, the results meet strong agreement with experiments.

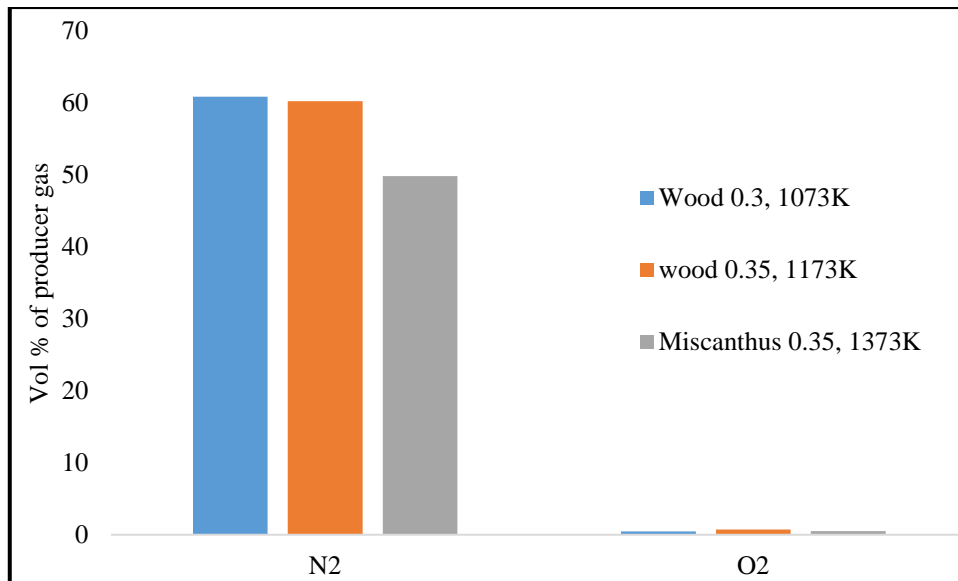


Figure 8: Oxygen and nitrogen concentrations with producer gas for different cases.

The set of results shown in Figure 8 illustrates nitrogen and oxygen concentrations (vol%), in producer gas. The results of different feedstocks. The results are average values recorded during experiments, and shows that oxygen is totally consumed or presents in negligible amounts, while nitrogen presents in values >50%. The results proves that gasification occurs during the experiment.

4.3 Total tar produced/100 ml of syngas

Tar produced from the model presents four main tar species, while the data from experiments introduce approximately twenty-six different aromatic and phenolic tar compounds. However, most of these compounds are negligible, and only a few of them have a considerable amount (Figure 4). Further, the basic reasons for choosing four main species in the modelling are that they represent the main tar species (primary, secondary and tertiary) in most cases at 70-95% of the tar produced from downdraft gasifiers. On the other hand, other tar products such as o-Xylene, Methylnaphthalene, and Acenaphthylene have no well-known chemical reaction kinetics although they still have considerable amounts in some cases.

4.4 Total tar amount for every run

The experiments were carried out at different temperatures varying between 1073 K and 1373 K for every feedstock, with three ERs (0.25, 0.3, and 0.35). Tar is collected first in 100 ml of syngas, as already shown in Figure 3(b), and every species in the samples is analysed and then the whole amount of tar for every sample is measured and recorded ($\text{g}_{\text{tar}}/\text{feed}$).

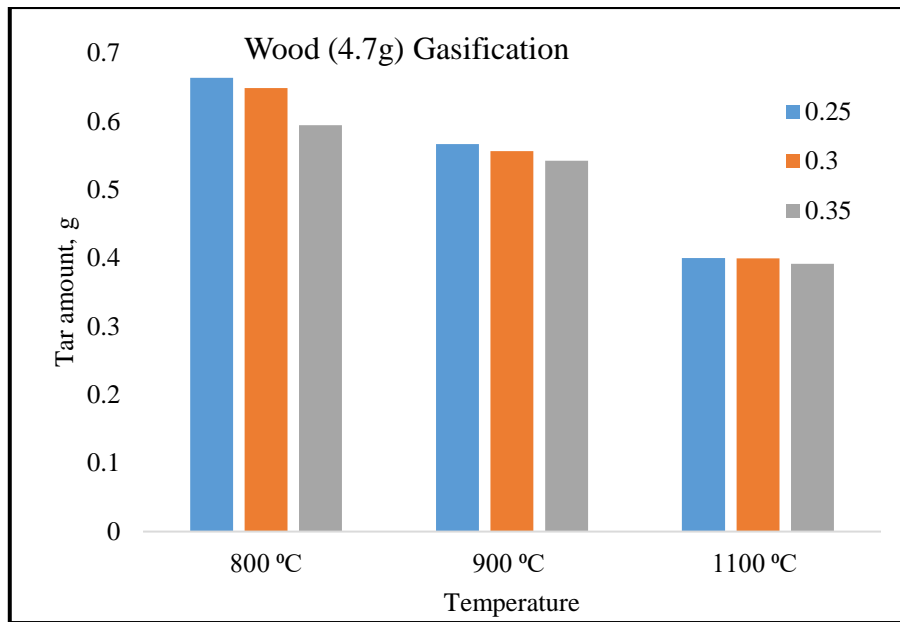


Figure 9. Total tar produced per sample with varying ER.

The results in Figure 9 reveal a decrease in the tar amount with increasing temperature or ER. Temperature increase encourages cracking reactions and, subsequently, increases their rates which lead to more cracking and a decrease in tar amount. On the other hand, higher ER leads to an increase in the amount of air (oxidant), which has the same effect of temperature and decreases the amount of tar. This finding also agrees with the previous researches e.g. [16], [11], [38], and [39], who reported a decrease of tar amount with the temperature and/or ER.

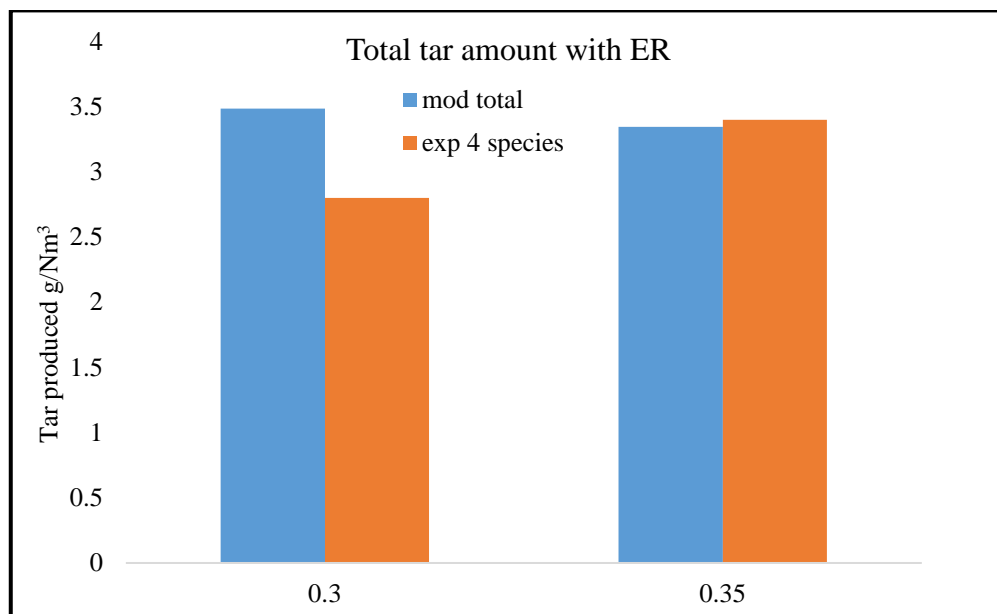


Figure 10. Comparison between the model and experiments for the total tar produced.

The results in Figure 10 show a comparison between the modelling and experimental data for the total tar produced. The comparison was made for the same ER, with a slight change in the temperature. For example, at ER 0.3, the model prediction is 1115 K, while the experiment was carried out at 1073 K. This might cause slight variations in tar produced as shown in Figure 10. However, at ER 0.35, the model and experiment were carried out at a similar temperature as shown in Figure 7, and therefore, the results tend to have a much better agreement. In the experiments, more than twenty different tar species were detected; however, as discussed earlier, only four main tar species were considered.

5. Sensitivity analysis

5.1. Moisture content effect on different gas species

The effect of changing moisture content on different gas species along the gasifier is addressed in the following sections. Results are derived from the kinetic model where the output from each zone is feeding to the next one. A loop calculation is made at every zone to calculate the exact temperature based on the energy balance and then the exact gas composition is measured.

Pyrolysis reactions are based on empirical correlations while combustion and reduction zones are based on the detailed kinetic rate reactions highlighted in [6], and other reactions as seen in Table 4.

5.1.1. Pyrolysis products

The results of different gas species and tar compounds were tested for different moisture content levels. The equivalence ratio has no effect on the pyrolysis temperature as the main factor at pyrolysis is the moisture content for specific feedstock and, therefore, the results of different gas species are the same as long as the temperature is constant. The results are discussed on the basis of one mole of biomass gasified. Tar products along the gasifier height will be discussed in a separate section because of their importance and also because tar amounts are small compared to other volatiles.

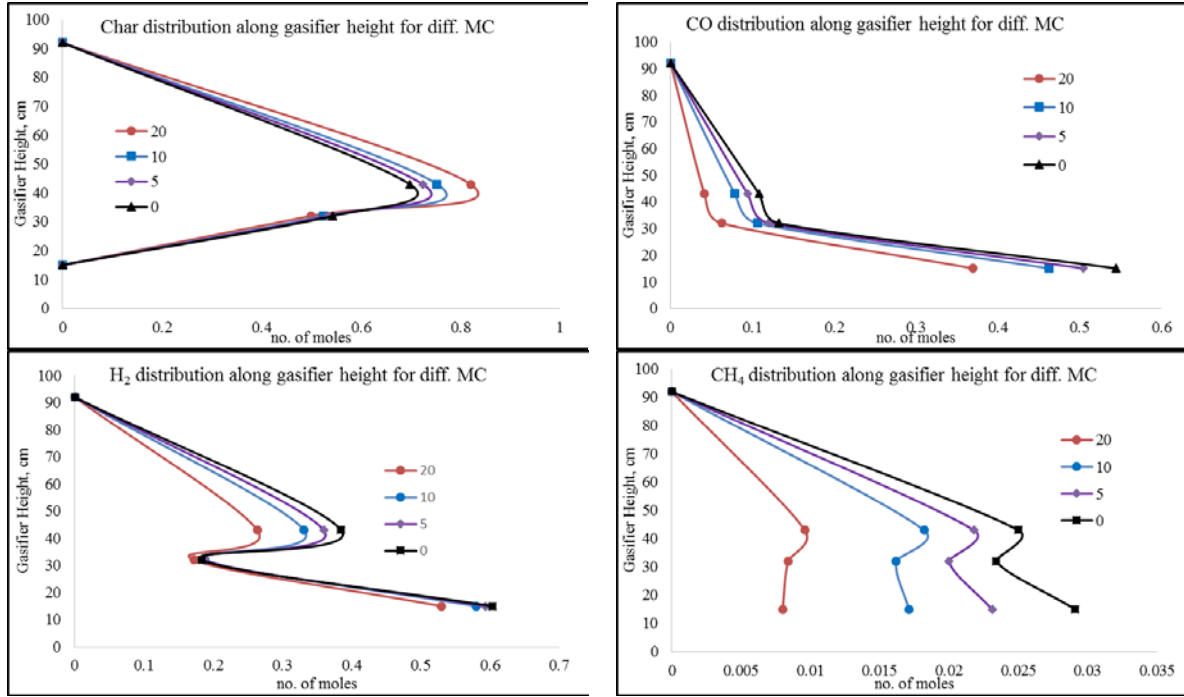
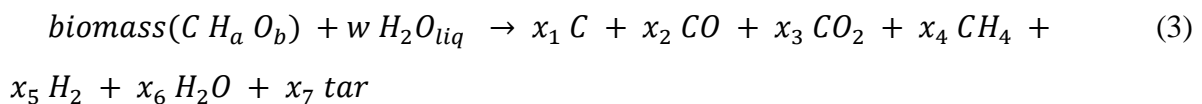


Figure 11: Different gas species variation along gasifier height with moisture content for wood pellets.

Figure 11 shows different gas species distribution along gasifier height with different MC levels, for wood pellets at a fixed ER of 0.27. Lower moisture content levels are favourable for the production of useful gas species (CO, H₂, and CH₄) and that is because higher moisture content levels tend to lower in other products. The biomass, after the drying process, decomposes into volatiles (CO, CO₂, CH₄, H₂, H₂O, and tar) and char. Based on Koufopanos [40], the biomass first decomposes into volatiles and char and then these components further react with each other to form more char and volatiles. Furthermore, based on the global reaction of pyrolysis (equation (3)), increasing moisture content tends to increase vapour in volatiles which affects other gases and consequently lowers them as shown in Figure 11. On the other hand, char was found to increase with moisture content, whereas the hydrogen and oxygen in biomass tend to be converted to volatiles including water vapour. The char included in biomass is converted to CO, CO₂, and a very small amount of tar. As long as the volatiles decrease, the amount of char will increase as shown in Figure 11.



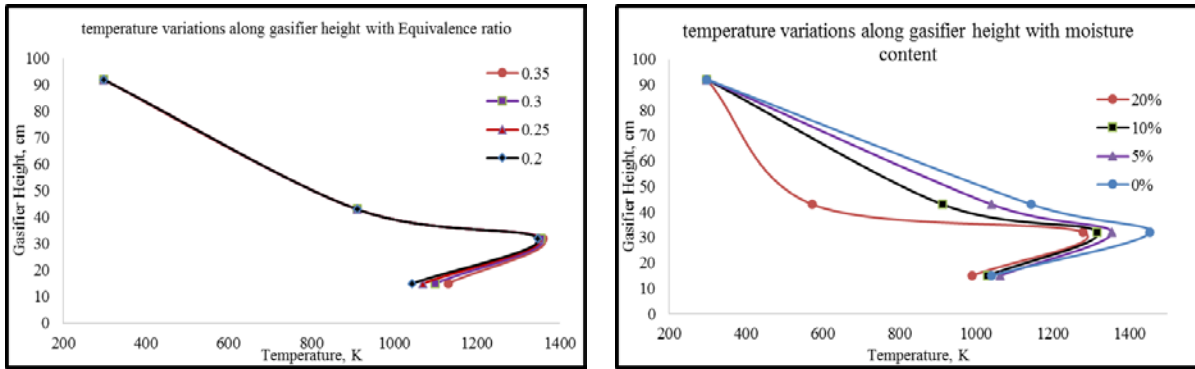


Figure 12: Temperature variation along gasifier height for wood pellets.

Temperature along the gasifier is calculated by the energy balance at the end of every zone. It is found that temperature drops along the gasifier as the moisture content levels in biomass increase (Figure 12). This is because higher water content in the feedstock requires more energy to remove and convert it to vapour and, therefore, the temperature decreases. The highest temperature is found to be 1410K, at MC=0% for wood pellets in the combustion zone, at ER of 0.27, while the lower temperature is at the pyrolysis zone, 732K, at 20% MC for the same feedstock and ER. Temperature variations along the gasifier height with varying ER are also studied for wood pellets at fixed MC=10%. Higher ER means more air addition, which increases the oxidation reactions (exothermic), thus resulting in more heat release and subsequently increasing the temperature inside the gasifier.

5.1.2. Combustion products

Increasing moisture content tends to increase vapour in volatiles which affect and decrease other gases and consequently reduces them as shown in Figure 11. Combustion reactions (Table 5) show higher rates for reactions 1, 2, and 3. Those reactions tend to rapidly increase all the H₂O and CO₂ levels during oxidation and this has a great effect on reducing H₂, and CH₄ levels. On the other hand, char is consumed in combustion forming CO, and CO₂ which lead to a reduction in char amount in the combustion zone. As shown in Figure 12, combustion temperature decreases with moisture content because higher moisture content levels affect gasifier temperature and tend to reduce it. Nitrogen concentration remains the same because the ER is constant, and the model does not take into account any NO_x formation or nitrogen reactions and conversion to other compounds.

Table 5: Oxidation Reactions ([41] and [42]).

	Reaction	A_j	E_j/R
1	$H_2 + 0.5 O_2 \leftrightarrow H_2O$	$1.6*10^9$	3420
2	$CO + 0.5 O_2 \leftrightarrow CO_2$	$1.3*10^8$	15106
3	$CH_4 + 1.5 O_2 \leftrightarrow CO + 2H_2O$	$1.585*10^9$	24157
4	$C + 0.5 O_2 \leftrightarrow CO$	0.554	10824

5.1.3. Reduction products

The results show a gradual increase for all gas products coming out of the reduction zone (Figure 11). Based on the reactions shown in Table 6, for reduction reactions, a higher reaction rate is found for reactions 1 and 2. Higher moisture content tends to increase CO, and H₂. However, the total amount of vapour is increasing and, therefore, reduces the final concentration of those gases. CH₄ was found to increase slightly depending on char and vapour concentration. Because the heating value depends on the amount of CO, H₂, and CH₄, it, therefore, reduces with moisture content increase. Moisture content levels are preferred to be low in order to achieve a higher heating value.

Table 6: Reduction Reactions [43] and [44].

	Reaction	A (1/s)	E (kJ/mol)
	Boudouard $C + CO_2 \leftrightarrow 2 CO$	36.16	77.39
	Water-gas $C + H_2O \leftrightarrow CO + H_2$	$1.517*10$	121.62
	Methane formation $C + 2H_2 \leftrightarrow CH_4$	$4.189*10$	19.21
	Steam Reforming $CH_4 + H_2O \leftrightarrow CO +$	$7.301*10$	36.15

Generally, from Figure 11, it can be concluded that H₂, and CH₄ are following similar trend. Both compounds starts formation in pyrolysis, and going through oxidation process leading to decrease because of combustion reactions and presence of O₂, then starts formation again in reduction zone because of methanation and water gas reactions. On the other hand char is formed during pyrolysis and been consumed in combustion and reduction zone because of oxidation reactions and the model already assumes total char consumption at reduction zone due to boundard, methanation, and water gas reactions.

5.2. Equivalence ratio effect on different gas species

Figure 13 illustrates the variation in different gas species along the gasifier height with a varying equivalence ratio. The calculations are carried out at a fixed MC of 10% for wood

pellets gasification. There is no variation in the pyrolysis zone as the MC is fixed and, therefore, pyrolysis temperature is constant as discussed earlier. A lower equivalence ratio tends to increase the rate of gasification reactions and reduces combustion reactions. Combustion reactions depend on the amount of air supplied which increases the formation of CO_2 and H_2O (Table 5). On the other hand more air supply will reduce useful gases (CO , H_2 , and CH_4) as a result of their oxidation and conversion to steam and CO_2 , while lower equivalence ratios tend to reduce the oxidation reaction rates. That might be a reason for increasing CO , H_2 , and CH_4 with a reduction in in CO_2 amounts. Lower equivalence ratios are favourable for the production of higher value producer gas. Higher values of char and syngas are found at lower ERs and the corresponding heating value is higher as well. Higher ER tends to increase oxidation temperatures and oxidation reactions that consume char and lead to the destruction of useful gases and increase water vapour and CO_2 .

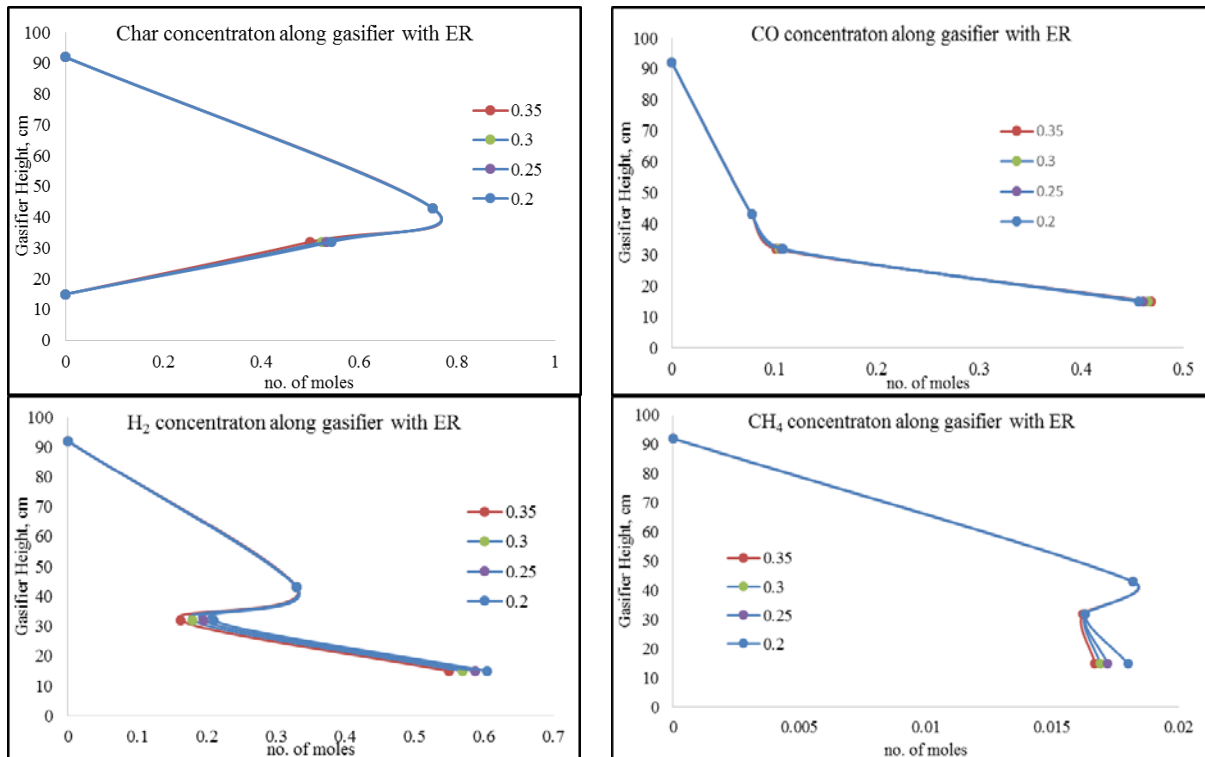


Figure 13: Equivalence ratio effect on different gas species along gasifier height for wood pellets at MC=10%

6. Tar species evolution and formation along gasifier

Tar species tracking from evolution at pyrolysis to combustion and reduction will be illustrated in the following sections.

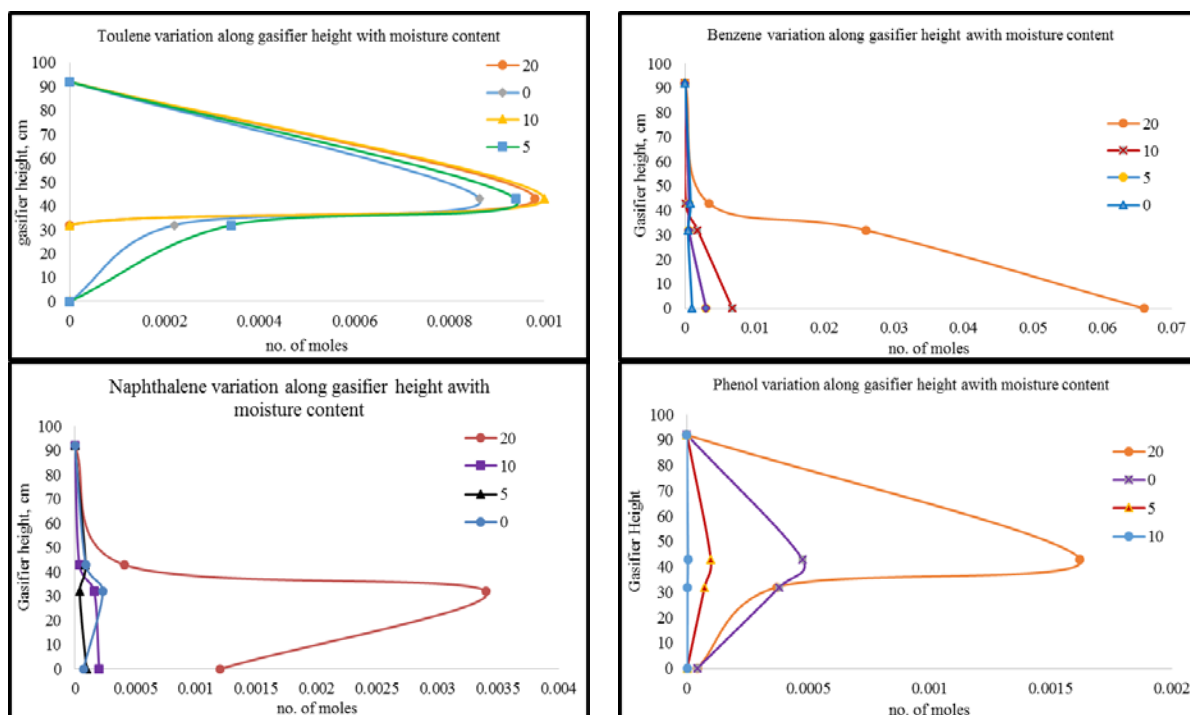


Figure 14: Tar evolution and formation along gasifier height at different moisture content levels.

Figure 14 illustrates the tar evolution along the different zones of the downdraft gasifier with fixed ER. Different tar species used in the model are traced from their formation in pyrolysis then combustion and reduction zone along gasifier height, depending on the temperature of each zone. The modeling was carried out at a fixed ER of 0.326, and with varying moisture content to study its effect on tar formation and to obtain the optimum conditions for less tar amount coming with producer gas. Phenol starts forming in pyrolysis and then a reduction in oxidation tends to disappear or to exist in very small amounts in producer gas; that is because it is a primary tar compound. Primary tars starts to form at temperatures 673-973 K [39] and, at temperatures above 773 K, primary tars starts reforming [45] and are converted to secondary then tertiary tars. The temperature profile along the gasifier within different moisture content or equivalence ratio is shown in Figure 12. Temperatures of oxidation and reduction zone that are higher than 1173 K are enough to destroy primary tar species and transform them into other compounds.

Toluene formation along the gasifier has the same trend of phenol, higher concentration in pyrolysis zone, followed by destruction in oxidation and reduction zone. Temperatures above 1173 K are enough to crack all phenol and toluene and convert them into benzene and other lighter species [1].

Naphthalene formation follows a different trend from other species. It is formed and is present in considerable amounts in producer gas. Small amounts are produced during

pyrolysis because it is a tertiary tar which requires higher temperatures to present and form. Higher temperatures in oxidation zone $>1300\text{K}$ are favourable for naphthalene formation which starts conversion for temperatures greater than 1300K and achieves total conversion at 1600 K [46]. Based on reactions 2 and 3 in Table 4, naphthalene is converted to char, H_2 , CO and benzene. Those reactions tend to take place in the combustion and reduction zones; however, it is more likely to happen in the reduction zone because of the presence of water vapour. Higher concentration of naphthalene in the oxidation zone is mainly a result of the conversion of lighter species (phenol and toluene) and also because of oxidation temperature which is in the ideal range of naphthalene formation and never exceeds the destruction temperatures ($>1600\text{ K}$).

Benzene has the highest portion of tar species, which is usually greater than 37% from the weight of total tars produced [2]. The results show a different trend of benzene formation and evolution from other species. Small amounts are formed in pyrolysis and then start to increase in the oxidation and reduction zone. Oxidation reactions tend to destroy benzene and convert it to CO , CO_2 , CH_4 , H_2 and H_2O . On the other hand these reactions depend on oxygen amount and have small reaction rates which make it unlikely that it will take place in the oxidation zone, and will never happen in the reduction zone where no oxygen is present. Other tar species (phenol, naphthalene, and toluene) are converted under this temperature range to benzene and other compounds. In addition, benzene conversion requires very high temperatures to take place $1400\text{-}1700\text{ K}$ [46]. The temperature along the gasifier shows the maximum temperature for the oxidation zone $<1500\text{ K}$, which is not enough to convert benzene to other species. All the previous factors tend to increase the amount of benzene along the gasifier height with an increase in temperature which agrees with the results of [1].

Higher moisture content levels tend to increase water vapour and hydrogen which favour tar formation reactions. Also, taking into account that higher moisture levels tends to reduce the temperature along the gasifier has a great effect on tar destruction which is favourable in higher temperatures.

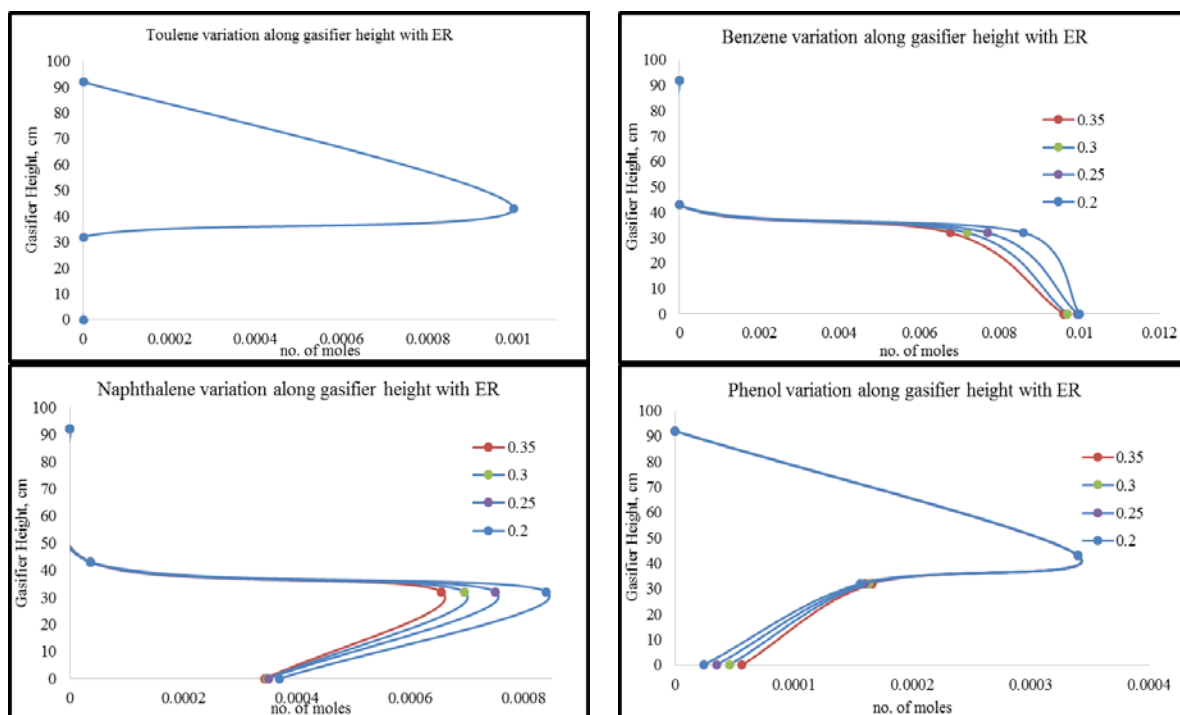


Figure 15: Tar evolution and formation along gasifier height at different moles equivalence ratio.

The results shown in Figure 15 demonstrate the effect of the equivalence ratio on tar evolution along different zones of downdraft gasifier. Rubber wood was used as feedstock with a moisture content of 10%. The same trend shown with varying moisture content also noticed with equivalence ratio. All tar species' evolution starts from pyrolysis.

Toluene behaviour is not affected by varying ER. As moisture content is fixed, the highest amount of toluene is formed during pyrolysis and is totally destroyed and converted to other compounds in the oxidation zone. This is because moisture content is the major factor affecting pyrolysis temperature and whether all tar compounds are derived through these relationships, depends on temperature (Table 3); therefore its amount will remain the same in pyrolysis. The amount of all four tar species used in the model is the same in pyrolysis. Oxidation temperature for different moisture content levels is greater than 1173 K, which is enough to convert all toluene amounts to other tar species and small amounts of lighter compounds (CO , H_2 , and CH_4). Phenol follows the same trend as toluene with small amounts starting to form again in the reduction zone as the temperature drops.

Naphthalene formation was found to have relatively high amounts compared to toluene and phenol, following the same trend as the changing moisture content effect. The temperature of oxidation and reduction has a major effect alongside the amount of water vapour, phenol, and toluene that are converted to naphthalene depending on their amount and reaction rates.

Benzene has the biggest portion of tar produced during biomass gasification. The results of changing moisture content or equivalence ratio show the same trend and find good agreement with other previous works such as [46], [47], [8] and [33]. For benzene, as moisture content decreases, the temperature increases, which is favourable to converting other gas and tar species to benzene. So benzene increases with the temperature which found good agreement with [46], and [1]. They showed that benzene formation increases with the temperature, and also benzene destruction starts after 1400K, which is almost the highest temperature in the current results at oxidation zone at 0% MC.

7. Conclusion

A novel and unique kinetic code was built to simulate downdraft gasifiers including detailed tar species and gas species formation along gasifier height and gasifier design. The data simulated by the current model has never been highlighted nor introduced in a single kinetic model, according to the research carried out in this paper.

The current research work is a combination of kinetic modelling for tar species formation and experimental work validation. The detailed kinetic code is based on eighteen different kinetic rate reactions for greater accuracy and prediction of tar evolution, formation and cracking throughout the different zones of downdraft gasifiers. The model is verified and found good agreement for wood biomass materials. The current model is used to address the evolution of different gas species, char and tar species along the gasifier, starting from the devolatilization process to combustion and reduction. Modelling, as well as experiments carried out by the paper's authors, shows good agreement and proves the model's stability and ability in order to predict the tar species produced from the wood downdraft gasifiers. The four main tar species were found to be a good representative for the tar evolution in the downdraft wood gasifiers, and in most cases, they form 50-90 % of the total tar produced. Sensitivity analyses were carried out at a different moisture contents and ER levels to address the optimum working conditions for the production of a higher value syngas with a lower tar amount. Using an equivalence ratio of 0.3, with lower values of moisture content < 10% will increase the yield of syngas, leading to an increase in the heating value with reasonable amounts of tar content in the producer gas.

Future work on the model will try to address and add more tar species which were found in significant amounts in the experiments.

ACKNOWLEDGMENT

The first author would like to thank the Egyptian Cultural Affairs and Missions Sector and the British Embassy in Egypt for funding his PhD research study at the University of Glasgow. He would also like to thank the University of Glasgow for funding mobility scholarship which supported the experimental work at the KTH institute, Sweden. The third author (M. C. Paul) acknowledges his RAEng/The Leverhulme Trust Senior Research Fellowship support (LTSRF1718\14\45) from the Royal Academy of Engineering, UK.

References

- [1] C.M. Kinoshita , Y. Wang, and J. Zhou, “Tar formation under different biomass gasification conditions,” *Journal of Analytical and Applied Pyrolysis*, vol. 29, pp. 169-181, 1994.
- [2] Basu P., Biomass Gasification, Pyrolysis, and Torrefaction. Practical Design and Theory. Second Edition, Amsterdam: Academic Press, 2013.
- [3] A.M. Sepe, J. Li, and M.C. Paul, “Assessing biomass steam gasification technologies using a multi-purpose model,” *Energy Conversion and Management*, vol. 129, pp. 216-226, 2016.
- [4] L. Yan, Y. Cao, and B. He, “On the kinetic modeling of biomass/coal char co-gasification with steam,” *Chem. Eng. J.*, vol. 331, pp. 435-442, 2018.
- [5] Y. Qin, A. Campen, T. Wiltowski, J. Feng, and W. Li, “The influence of different chemical compositions in biomass on gasification tar formation,” *Biomass and Bioenergy*, vol. 83, pp. 77-84, 2015.
- [6] A.M. Salem, and M.C. Paul, “An integrated kinetic model for downdraft gasifier based on a novel approach that optimises the reduction zone of gasifier,” *Biomass and Bioenergy*, vol. 109, pp. 172-181, 2018.
- [7] C.F. Palma, “Model for Biomass Gasification Including Tar Formation and Evolution,” *Energy and Fuels*, vol. 27, no. 5, pp. 2693-2702, 2013.
- [8] A. Dufour, L. Abdelouahed, O. Authier, G. Mauviel, J. P. Corriou, and G. Verdier, “Detailed Modeling of Biomass Gasification in Dual Fluidized Bed Reactors under Aspen Plus,” *Energy and Fuels*, vol. 26, pp. 3840-3855, 2012.
- [9] U. Kumar and M.C. Paul, “CFD modelling of biomass gasification with a volatile break-

- up approach,” *Chemical Engineering Science*, vol. 195, pp. 413-422, 2019.
- [10] C. Chen, M. Horio, and T. Kojima, “Numerical simulation of entrained flow coal gasifiers. Part I: modeling of coal gasification in an entrained flow gasifier,” *Chemical Engineering Science*, vol. 55, pp. 3861-3874, 2000.
- [11] A. Melgar, J.F. Pe´rez, H. Laget, and A. Horillo, “Thermochemical equilibrium modelling of a gasifying process,” *Energy Conversion and Management*, vol. 48, pp. 59-67, 2007.
- [12] P.P. Dutta, V. Pandey, A.R. Das, S. Sen, and D.C. Baruah., “Down Draft Gasification Modelling and Experimentation of Some Indigenous Biomass for Thermal Applications,” *Energy Procedia*, vol. 54, p. 21 – 34, 2014.
- [13] K.T. Wu, and R.Y. Chein, “Modeling of Biomass Gasification with Preheated Air at High Temperatures,” in *The 7th International Conference on Applied Energy*, 2015.
- [14] S.A. Channiwala, J.K. Ratnadhariya., “Three zone equilibrium and kinetic free modeling of biomass gasifier – a novel approach,” *Renewable Energy*, vol. 34, no. 4, p. 1050–1058, 2009.
- [15] Li XT, J.R. Grace, C.J. Lim, A.P. Watkinson, H.P. Chen, and J.R. Kim, “Biomass gasification in a circulating fluidized bed.,” *Biomass and Bioenergy*, p. 171–193, 2004.
- [16] A. Dufour, S. Valin, P. Castelli, S. Thiery, G. Boissonnet, A. Zoulalian, and P. Glaude, “Mechanisms and Kinetics of Methane Thermal Conversion in a Syngas,” *Ind. Eng. Chem. Res.*, vol. 48, no. 14, pp. 6565-6572, 2009.
- [17] A. M. Salem, U. Kumar, A. N. Izaharuddin, H. Dhimi, T. Sutari, and M. C. Paul, “Advanced numerical methods for the assessment of integrated gasification and CHP generation technologies,” in *Coal and Biomass Gasification*, Springer, (doi:10.1007/978-981-10-7335-9_12), 2018, pp. 307-330.
- [18] U. Kumar, A. M. Salem, and M. C. Paul, “Investigating the thermochemical conversion of biomass in a downdraft gasifier with a volatile break-up approach,” in *9th International Conference on Applied Energy (ICAE2017)*, Cardiff, UK, 21-24 Aug 2017.
- [19] K. Maniatis, “Introduction: tar protocols. IEA gasification,” *Biomass Bioenergy*, vol. 18, pp. 1-4, 2000.
- [20] R. Bridgewater, and A. Shand, “Fuel gas from biomass: Status and new modeling approaches,” *Thermochemical Processing of Biomass*, pp. 229-254, 1984.

- [21] S. Liu, D. Mei, L. Wang, and X. Tu , “Steam reforming of toluene as biomass tar model compound in a gliding arc discharge reactor,” *Chemical Engineering Journal*, vol. 307, p. 793–802, 2017.
- [22] B. Zhao, X. Zhang, L. Chen, R. Qu, G. Meng, X. Yi, and L. Sun, “Steam reforming of toluene as model compound of biomass,” *Biomass and Bioenergy*, vol. 34, pp. 140-144, 2010.
- [23] P. Ji, W. Feng, and B. Chen, “Production of ultrapure hydrogen from biomass gasification with air,” *Chemical Engineering Science*, vol. 64, no. 3, pp. 582-592, Feb, 2009.
- [24] J. Corella, M. A. Caballero, M. P. Aznar, and C. Brage, “Two advanced models for the kinetics of the variation of the tar composition in its catalytic elimination in biomass gasification,” *Ind Eng Chem Res*, vol. 42, pp. 3001-3011, 2003.
- [25] C. Di Blasi, “Modeling chemical and physical processes of wood and biomass pyrolysis,” *Progress in Energy and Combustion Science*, vol. 34, pp. 47-90, 2008.
- [26] C. Li, and K. Suzuki, “Tar property, analysis, reforming mechanism and model for biomass gasification—An overview,” *Renewable and Sustainable Energy Reviews*, vol. 13, pp. 594-604, 2009.
- [27] N. Bianco , M.C. Paul, G.P. Brownbridge , D. Nurkowski, A.M. Salem, U. Kumar, A.N. Bhave, and M. Kraft, “Automated Advanced Calibration and Optimization of Thermochemical Models Applied to Biomass Gasification and Pyrolysis,” *Energy and Fuels*, vol. 32, no. 10, pp. 144-153, 2018.
- [28] J. Yu, Experimental and Numerical Investigation on Tar Production and Recycling in Fixed Bed Biomass Gasifiers, Missouri University of Science and Technology, USA: ISBN: 9780438114807, 2018, PhD thesis.
- [29] Swedish Cleantech, “Belab AB,” [Online]. Available: <https://swedishcleantech.com/companies/1089/belab-ab/>. [Accessed 2019].
- [30] Verdant Chemical Technologies, “SPA – Offline tar analysis,” 2018. [Online]. Available: <http://www.verdchem.se/technology/spa-off-line-tar-analysis/>.
- [31] A. M. Salem, U. Kumar, and M. C. Paul, “Kinetic Modelling for Tar Evolution and Formation in a Downdraft Gasifier,” in *World Congress on Engineering*, London, UK, 04-06 July, 2018, pp. 800-804. ISBN 9789881404893.

- [32] A. Dufour, E. Masson, P. Girods, Y. Rogauze, and A. Zoulalian, "Evolution of Aromatic Tar Composition in Relation to Methane and Ethylene from Biomass Pyrolysis-Gasification," *Energy and Fuels*, vol. 25, p. 4182–4189, 2011.
- [33] D. Fuentes-Cano, A. Gómez-Barea, S. Nilsson, and P. Ollero, "Kinetic Modeling of Tar and Light Hydrocarbons during the Thermal Conversion of Biomass," *Energy and Fuels*, vol. 30, pp. 377-385, 2016.
- [34] F. Marias, A. Fourcault, and U. Michon, "Modelling of thermal removal of tars in a high temperature stage fed by a plasma torch," *Biomass and Bioenergy*, vol. 34, pp. 1363-1374, 2010.
- [35] P. Morf, P. Hasler, and T. Nussbaumer, "Mechanisms and kinetics of homogeneous secondary reactions of tar from continuous pyrolysis of wood chips," *Fuel*, vol. 81, pp. 843-853, 2002.
- [36] C. Gai, and Y. Dong, "Experimental study on non-woody biomass gasification in a downdraft gasifier," *International Journal of Hydrogen Energy*, vol. 37, pp. 4935-4944, 2012.
- [37] P. N. T. Hasler, "Gas cleaning for IC engine applications from fixed bed biomass gasification," *Biomass and Bioenergy*, vol. 16, pp. 385-395, 1999.
- [38] P. Morf, P. Hasler, and T. Nussbaumer, "Mechanisms and kinetics of homogeneous secondary reactions of tar from continuous pyrolysis of wood chips," *Fuel*, vol. 81, no. 7, pp. 843-853, 2002.
- [39] C. F. Palma, "Modelling of tar formation and evolution for biomass gasification: A review," *Applied Energy*, vol. 111, p. 129–141, 2013.
- [40] C.A. Koufopanosi, G. Maschio, and A. Lucchesi, "Kinetic Modelling of the Pyrolysis of Biomass and Biomass Components," *The Canadian Journal of Chemical Engineering*, vol. 67, pp. 75-84, Feb, 1989.
- [41] A.K. Sharma, "Modeling and simulation of a downdraft biomass gasifier 1. Model development and validation," *Energy Conversion and Management*, vol. 52, p. 1386–1396, 2011.
- [42] F.V. Tinaut, A. Melgar, J.F. Pérez, and A. Horrillo, "Effect of biomass particle size and air superficial velocity on the gasification process in a downdraft fixed bed gasifier. An experimental and modelling study," *Fuel Processing Technology*, vol. 89, p. 1076–1089, 2008.

- [43] D.L. Giltrap, R. McKibbin, and G.R.G. Barnes, "A steady state model of gas-char reactions in a downdraft biomass gasifier," *Solar Energy*, vol. 74, p. 85–91, 2003.
- [44] C.M. Kinoshita, and Y. Wang, "Kinetic Model of Biomass Gasification," *Solar Energy*, vol. 51, no. 1, pp. 19-25, 1993.
- [45] P. Basu, *Biomass gasification and pyrolysis: practical design and theory.*, Burlington: Academic press, 2010.
- [46] A. Jess, "Mechanisms and kinetics of thermal reactions of aromatic hydrocarbons from pyrolysis of solid fuels," *Fuel*, vol. 75, no. 12, pp. 1441-1448, 1996.
- [47] A. Fourcault, F. Marias, and U. Michon, "Modelling of thermal removal of tars in a high temperature stage fed by a plasma torch," *Biomass and Bioenergy*, vol. 34, pp. 1363-1374, 2010.

